Animal-associated marine Acidobacteria with a rich natural-product repertoire

Journal Article

Author(s):
Leopold-Messer, Stefan; Chepkirui, Clara; Mabesoone, Mathijs F.J.; Meyer, Joshua; Paoli, Lucas Pierre Antoine; Sunagawa, Shinichi; Uria, Agustinus R.; Wakimoto, Toshiyuki; Piel, Jörn

Publication date:
2023-12-14

Permanent link:
https://doi.org/https://doi.org/10.3929/ethz-b-000648878

Originally published in:
Chem 9(12), https://doi.org/10.1016/j.chempr.2023.11.003

Funding acknowledgement:
- PrediKSion: An evolutionary guided and experimentally validated computational pipeline to unravel new polyketide synthase functionality ()
- Tailored chemical complexity through evolution-inspired synthetic biology ()
- Investigating ribosomal peptide natural products in microbial dark matter of marine sponges ()

Animal-associated marine Acidobacteria with a rich natural product repertoire

Stefan Leopold-Messer[1,4], Clara Chepkirui[1,4], Mathijs F.J. Mabesoone[1], Joshua Meyer[1], Lucas Paoli[1], Shinichi Sunagawa[1], Agustinus R. Uria[2], Toshiyuki Wakimoto[2], Jörn Piel[1,3*]

[1]Institute of Microbiology, Eidgenössische Technische Hochschule (ETH) Zürich, Vladimir-Prelog-Weg 4, 8093 Zürich, Switzerland

[2]Laboratory of Natural Product Chemistry, Faculty of Pharmaceutical Sciences, Hokkaido University, Japan

[3]Lead contact

[4]These authors contributed equally

*Correspondence: jpiel@micro.biol.ethz.ch

SUMMARY

Sponges are well-known as rich sources of bioactive natural products. Various studies suggest that many of these compounds are produced by symbiotic bacteria. However, substance supplies and functional insights about the producers remain limited because cultivation remains unsuccessful. To identify alternative, sustainable sources of sponge-derived polyketides, we computationally analyzed 5289 characterized and orphan *trans*-acyltransferase polyketide synthases, enzymes with widespread roles in polyketide biosynthesis by bacterial symbionts. The workflow predicted marine animal-derived Acidobacteria of the family Acanthopleuribacteraceae with large sets of biosynthetic gene clusters to be enriched in sponge-type chemistry. Targeted compound isolation from a chiton-associated strain yielded new congeners of the phorboxazoles and calyculins, potent and scarce cytotoxins exclusively known from sponges, as well as the novel depsipeptides acidobactamides. These first natural products of Acidobacteria and new coral metagenomic data on a third family member suggest animal-associated Acanthopleuribacteraceae as a rich source of sponge-type as well as novel metabolites.

(Keywords: Natural products, Sponges, Bacteria, Polyketides, Genome mining, Symbiosis, Acidobacteria, Sustainable drug discovery)

INTRODUCTION

Marine invertebrates like sponges, tunicates, and bryozoans are prominent sources of bioactive natural products with therapeutic potential.[1,2] Commonly, the substances share structural characteristics of microbial natural products classes, including many compounds resembling complex polyketides (Figure 1). Examples are phorboxazole A (**1**) and spongistatin 1 (**2**) from sponges, exceedingly scarce and synthetically demanding polyketides that belong to the most potent antiproliferative agents reported to date.[3,4] In a growing number of cases, symbiotic bacteria have been demonstrated as the actual origin of invertebrate-derived natural products. Among the previously identified producers are members of the candidate genus 'Entotheonella' that synthesize numerous compounds in sponges, including calyculin A (**3**) and onnamide A (**4**) (Figure 1), 'Endolissoclinum faulkneri' producing patellazole B (**5**) in tunicates, and the bryostatin (**6**) producer 'Endobugula sertula' in bryozoans.[5-8] With the exception of a shipworm-associated bacterium,[9] none of the symbionts has, to our knowledge, been cultivated, but had to be identified by localizing the biosynthetic genes in cultivation-independent approaches, highlighting the difficulty to access these scaffolds with high novelty.

The growing evidence for widespread biosynthetic roles of symbionts offers major potential to identify and establish renewable bacterial production systems for rare and structurally distinct marine drug candidates. Besides cultivating producers, promising alternative avenues for biotechnological production are the expression of biosynthetic genes in surrogate hosts or the search for similar genes in cultivated bacteria.[10] However, none of these approaches are straightforward, with challenges including a limited access to invertebrates, the demanding and unpredictable heterologous expression of large polyketide synthase (PKS) and non-ribosomal peptide synthetase (NRPS) genes from non-standard bacteria, and biosynthetic genes that are often elusive or not clustered in biosynthetic gene clusters (BGCs) in symbionts.[8,11,12] As such, no broadly applicable method to facilitate access to symbiont-derived marine drug candidates has been established.

To address the challenge of sustainable production, we here asked whether alternative, cultivated producers for invertebrate natural products can be identified by *de novo* compound prediction from sequenced bacterial genomes, i.e., without prior knowledge of the symbiont genes. We focused on complex polyketides, which in non-actinomycete symbionts are predominantly generated by PKSs of the *trans*-acyltransferase (*trans*-AT) family.[13] A global bioinformatic analysis of orphan *trans*-AT PKSs in sequenced bacterial genomes revealed a metabolically rich acidobacterial taxon with a remarkably sponge-like chemical profile. We verified the predicted acidobacterial chemistry by isolating congeners of two rare families of complex marine polyketides as well as distinct depsipeptides from the bacterial cultures. With this, we also chemically validate Acidobacteria as an untapped, promising drug discovery source, and we highlight the use of global bioinformatic analyses of BGCs to identify and prioritize producers of novel scaffolds.[14]

RESULTS

Identification of phorboxazole-type polyketides

Trans-AT PKSs are multimodular enzymes containing unusually diverse biochemical features.[13,15-17] Even though they are widespread among bacteria and known to produce compounds of therapeutic value, many representatives occur in chemically poorly studied bacterial groups and are therefore underexplored.[13,18,19] Particularly striking is their prevalence in non-actinomycete symbiotic bacteria, in which they account for almost all complex polyketides with assigned biosynthetic genes.[11,13,20] Each module in a *trans*-AT PKS minimally contains, as integrated domains, an acyl carrier protein (ACP) that covalently binds a polyketide intermediate via a thioester moiety and a ketosynthase (KS) that performs intermediate chain elongation by adding an extension unit. This extension unit is usually derived from malonyl-CoA that is supplied by a *trans*-acting AT enzyme. Depending on a variable set of additional *cis*- and/or *trans*-acting biochemical components present in the upstream module, the structure of this incoming substrate can differ greatly in the α,β-region. We previously showed that these moieties tightly correlate with sequence features in the accepting downstream KS domains and can therefore be predicted with high confidence.[21] Concatenation of the chemical units predicted from all KSs in a *trans*-AT PKS then suggests the overall polyketide core structure, thus facilitating targeted polyketide discovery by genome mining.

Here, we tested a strategy to predict the production of sponge-type complex polyketides in cultivated bacteria. We first applied a computational analysis to identify architecturally unique *trans*-AT PKSs lacking assigned functions. Among these, we hoped to identify candidates for marine invertebrate-type polyketides by automated structural prediction. In this initial analysis, we processed all bacterial genomes published in the NCBI GenBank database between January 2021 and June 2022 through the BGC identification software antiSMASH.[22,23] Those BGCs classified as *trans*-AT type were combined with all *trans*-AT PKS BGCs deposited in the antiSMASH database (covering BGCs up to the year 2020), resulting in 5289 PKS pathways.[24] Each cluster was subsequently analyzed with an updated version of *trans*PACT,[25] which predicts KS substrates of *trans*-AT PKSs and infers a phylogenetic tree based on the KS patterns (Figure 2A). Mapping information on the genome source and on previously characterized PKSs onto these data then revealed functionally unassigned BGCs with unique architectures from cultivated bacteria for subsequent analysis by TransATor,[26] a computational tool that predicts chemical structures for *trans*-AT PKS products. Finally, the suggested structures of these orphan BGCs were subjected to substructure searches in the Dictionary of Natural Products,[27] PubChem,[28] and Reaxys.[29] In addition, structures were visually compared to a manually curated collection of polyketides reported from sponges and tunicates.[30]

Inspection of the phylogenetic tree inferred from the PKS domain sequences revealed multiple clades comprising PKSs of similar or identical architecture and assigned metabolites (Figure 2A). Disregarding clades with small PKSs comprised of 12 or fewer modules, the largest assigned clades were for bacillaenes, difficidins, rhizoxins, and oocydins (315, 134, 79, and 47 members, respectively). Conversely, several tree regions existed that mainly comprised metabolically unassigned and unique or rare *trans*-AT PKSs. To detect candidates for sponge-type pathways in free-living bacteria, we focused on such regions (Figure 2B) and PKSs from cultivated strains that were preferably available from strain collections. As first strong candidates based on TransATor predictions (see next section), we noticed two architecturally related hybrid *trans*-AT PKS-NRPS (*pho* and *phb*, Figure 2C) encoded in genomes of cultivated marine Acidobacteria of the family *Acanthopleuribacteraceae* (Figure 2C).[30,31] This was intriguing, since Acidobacteria are a diverse and ubiquitous, but functionally poorly characterized bacterial phylum with few cultivated members and no reported natural products. The candidate producers *Acanthopleuribacter pedis* FYK2218 and *Sulfidibacter corallicola* M133 have been isolated from a marine chiton[30] and a coral[31], respectively, and both contain large (>10 Mb) genomes.[31] The two strains comprise all presently available *Acanthopleuribacteraceae* genomes. AntiSMASH analyses indicated striking biosynthetic potential in both bacteria with at least 39 and 42 predicted BGCs, respectively (Figure 2D). In *A. pedis*, three of these BGCs belong to *trans*-AT PKS-NRPS hybrid systems, and a further PKS-NRPS BGC encodes *trans*-AT as well as *cis*-AT modules. For the initial chemical studies, we focused on the *pho* BGC (GenBank accession JAFREP010000003, Tables S1 and S2) from *A. pedis*.

Discovery of phorbactazole-type complex polyketides

The *pho* BGC from *A. pedis* encodes five PKS or PKS-NRPS proteins with a total of 26 modules (Table S1). TransATor-based structural predictions suggested a compound with two oxazole rings and three (partially) saturated pyran rings (Figure 3, Figure S1, and Table S2). Manual inspection did not suggest further structural changes except for a potential additional hemiacetal ring formed in the C-39 to C-43 region. Substructure searches in natural product databases using various portions of the prediction retrieved phorboxazoles as convincingly close hits (Figure 3A). Phorboxazole A (**1**) and congeners were first reported in 1995 by Searle and Molinski from a marine *Phorbas* sp. sponge collected off the Muiron Islands.[3] In 2004, Capon and coworkers also reported phorboxazoles from an Australian *Raspailia* sp. sponge.[32] With activity against all 60 tested cell lines of the National Cancer Institute (NCI) panel and mean growth inhibition (GI_{50}) values in the single-digit nanomolar range or lower, phorboxazoles are among the most potent known cytotoxins. The isolation from two taxonomically distinct sponges led to the speculation of a potential microbial phorboxazole producer, which to date remains unknown.

The bioinformatic prediction suggested a compound with a molecular formula of approximately $C_{55}H_{84}N_2O_{18}$ (calculated mass *m/z* 1060.5719 $[M+H]^+$), which we used as guidance for its targeted isolation from *A. pedis*. In contrast to most other Acidobacteria that are either fastidious or uncultivated, bacterial cultures grew rapidly. Following pilot cultivation in 20 mL of six different liquid media for three days, we extracted the supernatants with ethyl acetate and the cell pellets with a mixture of methanol and acetone (1:1) and subjected the residues to high-performance liquid chromatography-heated electrospray ionization-high resolution mass spectrometry (HPLC-HESI-HRMS, Figure S2). Analysis of the supernatant extracts revealed a candidate ion at *m/z* 957.4961 $[M+H]^+$, with a suggested molecular formula of $C_{50}H_{73}N_2O_{16}$ (Δ +0.64 mmu, Figure S3), close to the prediction. Furthermore, molecular network analysis[33] of the tandem MS (MS/MS) data showed that the detected ion was part of a larger cluster of ions (Figure S3). This cluster also contained ions at *m/z* 1000.5023 $[M+H]^+$ ($C_{51}H_{74}N_3O_{17}$; Δ +1.03 mmu), *m/z* 1119.5496 $[M+H]^+$ ($C_{56}H_{83}N_2O_{21}$; Δ +1.32 mmu) and *m/z* 1162.5554 $[M+H]^+$ ($C_{57}H_{84}N_3O_{22}$; Δ +1.30 mmu). The mass difference of 43 Da between the ions 957.5/1000.5 and 1119.5/1162.6 suggested congeners differing by one C, H, N, and O atom. Other ion pairs featured a 162 Da mass difference, indicating glycosylation by a hexose ($\Delta C_6H_{10}O_5$).

Cultivation of 20 L of *A. pedis* and repetitive MS-guided reverse-phase HPLC purification from organic extracts yielded six compounds, named phorbactazole A (**7**, 1.2 mg), B (**8**, 0.1 mg), C (**9**, 1.2 mg), D (**10**, 0.2 mg), E (**11**, 0.7 mg), and F (**12**, 0.9 mg) (Figure 3B). Compound **7** has the molecular formula $C_{51}H_{73}N_3O_{17}$ and 17 degrees of unsaturation deduced from the HRMS data (Figure S4). Analysis of the one- and two-dimensional nuclear magnetic resonance spectroscopy (NMR) data (Figure S5-S10 and Table S3) revealed three spin systems **I**-**III** (Figure S10) that were connected based on heteronuclear multiple bond correlations (HMBC) (see Supplemental Information). The relative configuration (marked by an asterisk) of four tetrahydropyran-type rings was assigned from NOESY data: ring A (5*R**, 6*S**, 7*R**, 9*S**), ring B (17*S**, *18R**, 19*R**, 21*S** or 17*S**, *18S**, 19*R**, 21*S** for compounds **8** and **10**), ring C (28*R**, 30*S**, 31*R**, 32*R**), and ring D (40*S**, 41*R**, 43*S**). The relative configuration of C12 was inferred from the nuclear Overhauser- effect (NOE) correlations along the spin system **I** as (12*S**). C-13, C-15, and the hemiacetal C-39 could not be stereochemically assigned by NMR (Figure S11). To obtain insights into the absolute configuration, sequence motifs of the ketoreductase (KR) domains[26] were analyzed, which in modular PKSs correlate well with the configuration of hydroxyl-bearing carbons.[34] The *pho* KRs (Table S2) suggested the following absolute configurations of oxygenbearing carbons: (7*R*, 9*S*, 13*R*, 15*R*, 19*R*, 21*S*, 30*S*, 32*S*, 41*R*, 43*S*). A complementary method to predict the absolute configuration is based on KS clades of *trans*-AT PKSs, and indicated (7*R*, 9*S*, 13*R*, 15*R*, 19*R*, 21*S*, 30*S*, 32*R*, 41*R*, 43*S*) (Table S2). The KR- and KS-based predictions agreed on all carbon centers of rings A, B, and D assignable by NMR, however for ring C only the KS-based prediction matched one of the NMR-elucidated enantiomers, with three axial protons (Figure S11C), rendering the KS-based prediction of C-32 more probable than the KR-based prediction. The combination of NMR and bioinformatic methods therefore suggest the absolute configuration of **7** as (5*R*, 6*S*, 7*R*, 9*S*, 12*S*, 13*R*, 15*R*, 17*S*, 18*S*, 19*R*, 21*S*, 28*R*, 30*S*, 31*R*, 32*R*, 40*S*, 41*R*, 43*S*) with only the hemiacetal C-39 unassigned (Figure 3B, Figure S10, Figure S11 and Table S2). [26,34]As predicted, compound **7** shares large molecular portions with the sponge-derived phorboxazoles.[3] The main differences to phorboxazoles are an expanded macrolide ring around C-10-17, a modified Western region that lacks the vinyl bromide moiety, and the presence of an *O*-carbamoyl substituent. Notably, our analyses also suggest an inverted absolute configuration of rings A and B, while the absolute configuration of rings C and D fits that reported for phorboxazole (Figure 3). However, these rings also carry different substituents, and the reported isolation and synthetic data suggest a correct assignment of the sponge compounds.[35]

NMR data for phorbactazole B (**8**) with the molecular formula $C_{50}H_{72}N_2O_{16}$ were similar to those of **7** (Figures S12-S16 and Table S3) but lacked signals for the carbamoyl unit (Figure 3B). Phorbactazole C (**9**, $C_{57}H_{83}N_3O_{22}$, Figure S17) yielded NMR spectra (Figures S18-S22 and Table S4) suggesting a glucose moiety attached to C-12 and carbamoylation at C-19 (Figure 3B, Figure S23). Phorbactazole D (**10**, $C_{56}H_{83}N_2O_{21}$, Figure S24) is a non-carbamoylated but glycosylated variant (Figures S25-S28 and Table S4). Two dehydration products of phorbactazole C, namely phorbactazole E (**11,** $C_{57}H_{81}N_3O_{21}$, Figure S29-S33 and Table S5) and phorbactazole F (**12,** $C_{56}H_{77}N_3O_{20}$, Figure S34-S38 and Table S5) were also isolated. Even though the two congeners were detected in the crude extracts, we could not rule out the possibility of them being degradation products from extraction process or the products of the isomerization observed in ring D (Figure S39). A comparison of the circular dichroism (CD) spectra of **7** with those of **8**-**12** suggested a similar configuration of all compounds, as the electronic circular dichroism (ECD) curves of these compounds were comparable in the range of 190-290 nm (Figure S40).

Biosynthetic model of phorbactazoles

A proposed model for phorbactazole biosynthesis is shown in Figure 4. The KS-based polyketide prediction and other components of the *trans*-AT PKS-NRPS proteins PhoA-E largely agree with the phorbactazole structures. The two NRPS modules and three PKS modules with pyran synthase (PS) domains positionally match the presence of two oxazoles and three pyran-type rings in phorbactazoles (rings A-C), with another six-membered ring (ring D) likely arising from spontaneous hemiketal formation. A discrepancy of the PKS architecture to the phorbactazole structures lies in the first PKS module, in which the KS domain seems to lack a function. Inspection of the KS protein sequence showed overall conserved active-site residues except for a Cys-to-Ser mutation of a site critical for chain elongation. Together with the phorbactazole structure, this suggests the KS decarboxylates a malonyl unit on the first module to generate an acetyl starter. In analogy to functionally related domains in many *cis*-AT PKSs named KS_Q due to a Gln mutation,[36] we termed the phorbactazole domain KS_S. Further, all phorbactazoles contain two off-pattern hydroxy groups at C-12 and C-18. In agreement, bimodules 15+16 and 19+20 of the *pho* PKS as well as the free-standing oxygenase PhoL match regarding architecture and protein homologies counterparts in the oocydin PKS (OocM) that we recently showed to install α-hydroxylations during chain elongation.[15] At the terminus of the assembly line, PhoE features an unusual architecture with internal TE and C domains. Internal TEs, for which we earlier proposed the term TE_B for branching thioesterase, are also present in several other *trans*-AT PKSs,[15] and for a TE_B of the oocydin PKS we showed that it installs an *O*-acetyl group.[17] A similar reaction in phorbactazole biosynthesis might facilitate elimination to generate the *Z*-configured double bond present at the biosynthetic polyketide terminus.[17] The *pho* BGC also contains the non-PKS genes *phoF* and *phoM* encoding a putative glycosyl and carbamoyl transferase, respectively, which match the glycosylation and carbamoylation substituents in phorbactazoles **7** and **9**-**12**. Although the *pho* architecture and phorbactazole structures are in good agreement, trials to genetically modify *A. pedis* for BGC inactivation have not yet been successful, and the biosynthetic model is therefore putative.

A second *trans*-AT PKS in *A. pedis* produces sponge-type calyculinamides

Further analysis of the TransPACT output revealed another gene cluster in *A. pedis*, termed *cly* BGC, that was strikingly similar to the calyculin (*cal*) BGC previously identified in an uncultivated

'Entotheonella' sp. symbiont of the sponge *Discodermia calyx* (Figure 2A, 5 and Figure S41).[6] Calyculins are highly potent phosphatase inhibitors[37] with picomolar inhibitory activity against several tumor cell lines.[38] Calyculin A (**3**) is employed as a cellular probe[39] and currently sourced from the sponge for commercial supply. The *cly* PKS architecture perfectly agrees with that of the calyculin PKS (*cal*) except for the additional presence of an *O*-methyl transferase domain between KS14 and 15 (Figure S41). HPLC-HESI-HRMS data of a 20 mL pilot extraction revealed a candidate ion at *m/z* 1041.5776 $[M+H]^+$, which had a suggested molecular formula of $C_{51}H_{86}N_4O_{16}P$ (Δ +0.55 mmu), differing from **3** by CH_4O (Figures S42 and S43). MS/MS fragmentation patterns and a GNPS library search supported the compound being related to the calyculin family (Figure S42).[33] For further insights into the identity of these compounds, we compared the bacterial extracts to those of the sponge *D. calyx* using molecular network analysis.[33] This showed a large cluster of ions shared between the two samples (Figure S42). Ions corresponding to reported calyculins A-J with nitrile moieties were only detected in the sponge. However, ions of similar *m/z* values and with matching MS/MS fragmentation patterns were located in both samples, suggesting closely related compounds.

To isolate the main compound (**13**), the supernatants of 12 L combined *A. pedis* cultures were extracted with ethyl acetate and subsequently separated by repetitive HPLC. MS-guided fractionation followed by structure elucidation (see Supplementary Information) yielded 0.2 mg of 21-methoxy calyculinamide A (**13)** (Figure 5, Figures S44-S50, Table S6-S8). While the NOESY data suggested the relative configuration of only the spirocyclic moiety, stereochemically informative features of the *cly* KS and KR domains perfectly matched those of the calyculin (**3**) PKS except for the KR between KS13 and 14. The combined bioinformatic data therefore suggested almost identical absolute configurations of **3** and **13** with an epimerized center at C-21 in **13** that is supported by the NMR data. In addition to this configurational difference, **13** but not **3** contains a methoxy group at C-21 that agrees with a unique *O*-methyltransferase domain located before KS15 in the *cly* PKS (Figure S41). A similar moiety at that position is found in the calyculin congeners geometricin[40] and swinhoeiamide[41] from sponges, for which the PKSs are unknown. These also harbor the same relative configuration of C-21 as **13**.

Further analysis of *A. pedis* cell pellets also revealed the ion *m/z* 1121.5449 $[M+H]^+$ with a suggested molecular formula of $C_{51}H_{87}N_4O_{19}P_2$ (Δ +0.94 mmu) corresponding to a variant of **13** with an additional phosphate group (Figure S51). Characteristic fragment ions are shared between this ion and compound **13**, corroborating related structures. Since this suggested phospho-21-methoxy-calyculinamide was present at minute amounts and highly unstable, isolation was not attempted.

Acidobactamides A-C (15-17), peptide-polyketide hybrids from *A. pedis*

To gather additional insights into the biosynthetic potential of Acanthopleuribacteraceae, we aimed to isolate and characterize further natural products of *A. pedis*. A multimodular biosynthetic system comprising nine NRPS modules interspaced by three PKS modules, termed *aba* (Figure S52, Table S9), was suggested by antiSMASH[42] and PRISM analysis[43] to synthesize a peptide containing a threonine unit (module 6 in Figure S52) that is extended by one PKS module (module 7 in Figure S52), resulting in a 4-amino-3,5-dihydroxy-2-methylhexanoic acid (Admha) motif (Figure 5, Figure S52-S53). This caught our attention, since a SciFinder[44] search revealed depsipeptides from marine sponges as the only other known natural products with a closely related, non-methylated variant of this moiety, a 4-amino-3,5-dihydroxyhexanoic acid (Adha) residue (Figure 5, Figure S53). These compounds are the cyclolithistides isolated from *Discodermia japonica*[45] and *Theonella swinhoei*[46], and phoriospongins from *Phoriospongia* sp. and *Callyspongia bilamellata*.[47] To isolate the predicted compound, NMR-guided isolation was adopted. A close look into the ^1H and HSQC NMR spectra (Figure S54-S55) of the crude extracts HPLC fraction F12 revealed the presence of proton signals attributed to the α-methines of amino acid residues (δ_H 3.9–5.0 ppm) and aromatic proton signals attributed to 1,4-disubstituted and benzene moieties (δ_H 6.9-7.31 ppm). MS analysis of this fraction revealed an ion at *m/z* 1343.6689 $[M+H]^+$ with a suggested molecular formula of $C_{62}H_{94}N_{12}O_{21}$ (Δ -3.244 mmu, Figure S56) Several rounds of purification and NMR-based structure elucidation yielded acidobactamide A (**15**, Figure 5, Figures S57-S81, Table S10-S12), a depsipeptide featuring several unusual residues: 3,6-diamino-5,7-dihydroxy-7-(4-methoxyphenyl)heptanoic acid (Ddmpha), the predicted Admha residue, 2-hydroxy-3-phenylpropanoic acid (Hppa), and *N*-methyl isoleucine (*N*-Me-Ile). Acidobactamide A (**15**) shares a central *N*-branched Ile-COO-Admha-Gly portion with the sponge-derived cyclolithistides (Figure 5) but differs in other molecular regions. A substructure search in natural product databases for the unusual Ddmpha residue yielded no results, and hence to our knowledge **15** is the first natural product containing this moiety.

Two additional congeners of **15**, acidobactamide B (**16**) and acidobactamide C (**17**) were characterized. The MS and NMR data of **16** (Figures S82-S90, Table S13), with the molecular formula $C_{63}H_{96}N_{12}O_{21}$, suggested a similar structure to **15** with an additional ß-methylation on the aspartic acid residue. Responsible for this modification might be one of the two cluster-encoded B_{12}-dependent radical *S*-adenosyl methionine methyltransferases, AbaH and AbaL (Figure S52, Table S9).[48] The MS and NMR data of acidobactamide C (**17**) (Figures S91-S99, Table S14), with the molecular formula $C_{61}H_{92}N_{12}O_{21}$, indicated that the central isoleucine of **15** is replaced by a valine in **17**. To identify candidate genes responsible for the β-hydroxylation of tyrosine in **15**-**17** we analyzed the protein AbaK using Phyre2.[49] Although the protein was genome-annotated as a metallohydrolase, two high-confidence Phyre2 hits were the amino acid β-hydroxylases FrsH and CmlA, which have been shown to act *in trans* on assembly line-bound substrates, suggesting a similar function for AbaK in tyrosine hydroxylation.[50,51] In summary, the acidobactamide (**15**-**17**) structures largely agree with the adenylation domain substrate selectivity and the PKS domain architecture of antiSMASH and PRISM predictions (Figures S52 and S53). For the two NRPS modules that had ambiguous predictions, Asp and Gln residues were elucidated from NMR data. Additionally, Marfey's analysis confirmed two D-configurated amino acids matching the presence of two epimerization (E) domains (Figure S52, Figure S100).

Bioactivity of phorbactazoles, 21-methoxy calyculinamide, and acidobactamides

Assays with phorbactazoles A-F (**7-12**) and Henrietta Lacks (HeLa) cervical cancer cells showed activity in the micromolar range for phorbactazoles A-F (IC_{50} 2.4, 10.2, 2.4, 3.2, 2.0, and 2.6 μM for **7**-**12**, respectively, Figure S101). These IC_{50} values are higher than those reported for phorboxazole A (**1**, IC_{50} < 1 nM) and comparable to hemi-phorboxazole A (IC_{50} > 10 μM), a shortened phorboxazole congener.[53] Structure-activity relationship studies on phorboxazoles have shown that the vinyl bromide and the diene group present in **1** but not in **7-12** are crucial for cytotoxicity in the low nM range.[54] Of specific interest are the C-1 to C-32 and C-1 to C-38 phorboxazole analogs (Figure 3A) synthesized by Uckun and Forsyth.[54] The IC_{50} values of these more phorbactazole-like analogs were outside the tested concentrations (IC_{50} > 2 μM) against various cancer cell lines. The carbamoylation of phorbactazole A (**7**) increases its cytotoxicity about 4-fold compared to phorbactazole B (**8**). Carbamoylation has been reported to increase potency of other natural products.[55,56] Assay data of phorbactazole A (**7**) and C (**9**) indicate that the glycosylation does not influence activity. We also tested 21-methoxy calyculinamide (**13**) in this assay, which revealed potent activity at an IC_{50} of 0.3 nM, similar to calyculins and calyculinamides.[57,58] Acidobactamides A-C (**15**-**17**) showed moderate cytotoxicity (IC_{50} 15.0, 21.4, and 13.9 μM for **15**-**17**, respectively, Figure S101). Compounds **7**-**10, 13** and **15**-**17** were also evaluated for antimicrobial activity against a panel of bacteria (Table S15). Compounds **7**-**10** and **13** did not exhibit activities at concentrations ≤100 mg/mL, while **15**-**17** were inactive at any of the tested concentrations (≤50 mg/mL).

Natural product richness and animal-associated lifestyle of Acanthopleuribacteraceae

The BGC-rich *Acanthopleuribacteraceae* members *A. pedis* and *S. corallicola* have been isolated from the chiton *Acanthopleura japonica* and the coral *Porites lutea*, respectively.[31] Based on genome features of these strains and on the detection of sequence reads from uncultivated members of this family in further animal microbiomes, an animal-associated lifestyle was suggested for this acidobacterial family.[31] To evaluate whether *A. pedis* may be more consistently associated with the chiton rather than being a transitory colonizer, we recollected the chiton *A. japonica* at the same location reported in the 2008 isolation study.[30] The presence of *A. pedis* in the chiton was assessed through the workflow described in Figure S102. We isolated high-molecular weight metagenomic DNA from six collected chiton samples. Using primers designed based on the 16S rRNA gene sequence of *A. pedis* (GenBank accession number NR_041599.1), we performed PCR experiments with each purified DNA sample as template. DNA electrophoresis showed correct-sized amplicons of ~1.4 kb in five of the six different metagenome samples, but not in negative controls (Figure S102 and Tables S16 and S17). Sequencing of cloned PCR products from two samples showed 100% sequence identity with the 16S rRNA gene sequence of *A. pedis* for one sample and a single point mutation for the other (Table S16, 17). This suggests that *A. pedis* is more commonly and over larger time scales associated with specimens of the chiton collected at Chiba (Figure S102 and Tables S16 and

S17). We were not able to detect compounds **7**-**13** and **15**-**17** in the animal extracts. Further studies are required to characterize the nature of this association.

The results on *A. pedis* and *S. corallicola*, the only two *Acanthopleuribacteraceae* members for which genomic data are available, motivated us to perform a targeted search for additional representatives in metagenomic datasets as described before.[59] For a metagenome from the coral *Millepora platyphylla* collected at the *Tara Pacific* expedition (Figure 6A, TARA_CO-0003230_METAG), we were able to reconstruct a metagenome-assembled genome (MAG) of a further member that belong to an unassigned *Acanthopleuribacteraceae* genus according to phylogenetic analyses (Supplementary Information, Figure 6A). The genome of approximately 7.3 Mb was estimated as 91.88% complete with 0.85% contamination (Supplementary Information) and good integrity (79 scaffolds, longest scaffold >370 kb, N50 ~150 kb). Using antiSMASH we identified 39 BGC-containing scaffolds of which at least 7 belonged to *trans*-AT PKSs (Figure 6C). In total, 69 KS domains of modular PKSs and 156 adenylation domains of NRPSs were detected (Figure 6). A TransPACT analysis was performed to estimate the diversity of the *trans*-AT PKSs in the three genomes (Figure 6D). None of the *trans*-AT PKS BGCs are architecturally identical between the three bacteria. Qualitative analysis of the *Millepora* MAG BGCs suggest complex biosynthetic pathways, of which two architecturally unusual *trans*-AT PKS-NRPS hybrids are shown in Figure 6E. These data corroborate the impressive BGC richness and common animal-associated lifestyle of this acidobacterial family.

DISCUSSION

Acidobacteria are a large and abundant bacterial phylum with members detected in diverse habitats.[12,14,30,31,61] In studies on different soil environments, Acidobacteria comprised on average ca. 20% of the total bacterial communities.[62,63] Despite their ubiquitous occurrence, only few members of this phylum have been cultivated, with *A. pedis* reported in 2008 as only the fourth cultured representative.[30,64] Genome analyses of cultivated strains as well as metagenomic studies of soil communities have suggested rich biosynthetic potential for some Acidobacteria based on the presence of multiple NRPS, PKS, and further gene clusters.[14,65] However, to the best of our knowledge, no natural product has been reported to date from this phylum. In this work, we provide functional evidence for Acidobacteria as a rich and untapped natural product resource by isolating bioactive, complex polyketides as well as depsipeptides from three different *A. pedis* pathways. Our analysis suggests that most *trans*-AT PKSs present in currently available acidobacterial genomes are found in the talented natural product family of *Acanthopleuribacteraceae*. All three available *Acanthopleuribacteraceae* genomes, one a MAG reconstructed in this study, feature large numbers of BGCs suggesting a metabolic richness comparable to that of the industrially relevant streptomycetes.[66] In agreement, HPLC-MS profiling (Figure S2) and MS network analysis (Figure S3) revealed further metabolites unrelated to the compounds isolated here. These data suggest that targeted cultivation efforts to expand the number of available strains could be rewarded with a substantial number of bioactive compounds. Particularly remarkable is the resemblance of the isolated *A. pedis* compounds to those from currently uncultivated sponge symbionts, as well as the presence of a further variant of a phorboxazole-type BGC in *S. corallicola*. Such high frequency of sponge-type pathways in closely related bacteria is, to our knowledge, unprecedented and raises intriguing questions on the broader chemical diversity of this taxon, the ecological roles of the substances in host-bacterial interactions, and the evolutionary origin of the natural product pathways in sponge symbionts. In a previous study[31], GenBank entries with sequence reads with >92% identity to the 16S rRNA gene of *S. corallicola* and *A. pedis* were identified for microbiomes of corals (*P. lutea*, *Acropora eurystoma*) and fish (*Seriola rivoliana*). Our updated analysis that includes 16S rRNA genes above 90% identity retrieved further sequences from microbiomes of sponge, corals and the coccolithophore *Emiliania huxleyi* (Table S18). In addition, chiton recollection and reconstruction of a third *Acanthopleuribacteraceae* genome from the coral *M. platyphylla* corroborate a close association with marine animals.[31] However, the frequency and roles of symbiotic relationships in this Acidobacterial family and function of the metabolites in host-bacterial interactions remains to be studied.

The identification of alternative, cultivated bacterial sources has been a successful method to obtain polyketides and modified peptides from marine macroorganisms. Examples are swinholides[67], oocydins[68], lobatamides[69,70], didemnins[71], microsclerodermins[72], bengamides[73], and polytheonamides[10]. With the exception of the ribosomally synthesized polytheonamides[74], these previous cases were serendipitous discoveries. In this work we show that the TransPACT tool can pinpoint sustainable supplies of rare polyketides in a systematic, targeted fashion. This is feasible for substances with known biosynthetic genes, as demonstrated for calyculinamides, as well as through *de-novo* prediction from orphan BGCs aided by TransATor, as applied to phorboxazol-type polyketides. While the nonribosomal peptides in this study were isolated by individual BGC mining, the same large-scale methods as applied for polyketides might also be feasible for nonribosomal peptides, which are also generated by multimodular assembly lines well-suited for prediction. With the rapid increase of publicly available bacterial genomes, we anticipate that the mining strategy presented here will reveal sustainable sources for many further natural products.

EXPERIMENTAL PROCEDURES

Resource availability

Lead Contact

Further information and requests for resources and reagents should be directed to the lead contact, Prof. Jörn Piel (jpiel@micro.biol.ethz.ch).

Materials availability

Compounds generated in this study will be made available on request. All other materials are commercially available or can be prepared as described.

Data and code availability

All data supporting the findings of this study are included within the article and its Supplemental Information and are also available from the authors upon request. Scripts and sequencing data files used for bioinformatic analysis are available at *https://github.com/mathijs-m/transPACT_wrapper*. The phorbactazole, 21-methoxy calyculinamide, and acidobactamide BGCs have been deposited in MIBiG under accession no. BGC0002813, BGC0002814, and BGC0002815, respectively. Data underlying figures 2 and 6, and genomic information of the *M. platyphylla*-associated *Acantipleuribacteraceae* member is available in the Zenodo repository https://doi.org/10.5281/zenodo.8255904.

SUPPLEMENTAL INFORMATION

Supplemental Information can be found online at ###

ACKNOWLEDGEMENTS

We thank Kefu Yu and Guanghua Wang for insightful discussions and Hans-Joachim Ruscheweyh as well as the ETH IT team for their computational support. We also thank Dr. Kensuke Yanagi (Coastal Branch of Natural History Museum and Institute, Chiba) for his help in collecting the chitons. M.M. has received funding from the European Union's Horizon 2020 research and innovation programme under the Marie Skłodowska-Curie grant agreement No. 897571. J.P. acknowledges funding by the European Research Council (ERC) under the European Union's Horizon 2020 research and innovation program (grant agreement No 742739), the Gordon and Betty Moore Foundation (#9204, https://doi.org/10.37807/GBMF9204), the Swiss National Science Foundation (SNSF; 185077, 197245), and the ETH (Research Grant ETH-21 18-2). T.W. acknowledges funding by the JSPS KAKENHI (Grant numbers JP21H02635 and JP22H05128). A.U has received funding from the JSPS KAKENHI (Grant number JP 21K06612). J.P, T.W. and A.U. acknowledges the support of Global Station for Biosurfaces and Drug Discovery, a project of Global Institution for Collaborative Research and Education in Hokkaido University. S.S. acknowledges funding by the SNSF (205321_184955). We would like to thank the expedition participants and consortium partners of Tara Pacific (https://zenodo.org/record/3777760#.YfEEsfXMLjB), Eric Rottinger, Ryan McMinds, Cecile Rottier, and Claudia Pogoreutz for collecting samples, and Stéphane Pesant for curating the data of the coral-associated microbial genome presented in this study.

AUTHOR CONTRIBUTIONS

M.M. and S.L.-M. performed bioinformatic studies on polyketide predictions. S.L.-M. and C.C. isolated and characterized natural products. S.L.-M. and C.C. performed bioactivity assays. A.R.U. and T.W. sampled chitons and performed metagenomic analyses. L.P. and S.S. performed analyses of the Tara Pacific dataset and metagenomic genome reconstruction. S.L.-M and J.P. wrote the paper with contributions of all authors.

DECLARATION OF INTERESTS

The authors declare no competing interests.

INCLUSION AND DIVERSITY

One or more of the authors of this paper self-identifies as an underrepresented ethnic minority in science

.

REFERENCES

1. Han, B.-N., Hong, L.-L., Gu, B.-B., Sun, Y.-T., Wang, J., Liu, J.-T., and Lin, H.-W. (2019). Natural Products from Sponges. In Symbiotic Microbiomes of Coral Reefs Sponges and Corals, Z. Li, ed. (Springer), pp. 329-463. https://doi.org/10.1007/978-94-024-1612-1_15.
2. Fusetani, N., and Matsunaga, S. (1993). Bioactive Sponge Peptides. Chem. Rev. *93*, 1793-1806. https://doi.org/10.1021/cr00021a007.
3. Searle, P.A., and Molinski, T.F. (1995). Phorboxazoles A and B: Potent Cytostatic Macrolides from Marine Sponge *Phorbas* Sp. J. Am. Chem. Soc. *117*, 8126-8131. https://doi.org/10.1021/ja00136a009.
4. Pettit, G.R., Cichacz, Z.A., Gao, F., Herald, C.L., Boyd, M.R., Schmidt, J.M., and Hooper, J.N.A. (1993). Isolation and Structure of Spongistatin. J. Org. Chem. *58*, 1302-1304. https://doi.org/10.1021/jo00058a004.
5. Wilson, M.C., Mori, T., Rückert, C., Uria, A.R., Helf, M.J., Takada, K., Gernert, C., Steffens, U.A., Heycke, N., Schmitt, S., et al. (2014). An environmental bacterial taxon with a large and distinct metabolic repertoire. Nature *506*, 58-62. https://doi.org/10.1038/nature12959.
6. Wakimoto, T., Egami, Y., Nakashima, Y., Wakimoto, Y., Mori, T., Awakawa, T., Ito, T., Kenmoku, H., Asakawa, Y., Piel, J., and Abe, I. (2014). Calyculin biogenesis from a pyrophosphate protoxin produced by a sponge symbiont. Nat. Chem. Biol. *10*, 648-655. https://doi.org/10.1038/nchembio.1573.
7. Kwan, J.C., Donia, M.S., Han, A.W., Hirose, E., Haygood, M.G., and Schmidt, E.W. (2012). Genome streamlining and chemical defense in a coral reef symbiosis. Proc. Natl. Acad. Sci. U.S.A. *109*, 20655-20660. https://doi.org/10.1073/pnas.121382010.
8. Sudek, S., Lopanik, N.B., Waggoner, L.E., Hildebrand, M., Anderson, C., Liu, H., Patel, A., and Sherman, D.H.H., Margo G. (2007). Identification of the Putative Bryostatin Polyketide Synthase Gene Cluster from "*Candidatus* Endobugula sertula", the Uncultivated Microbial Symbiont of the Marine Bryozoan *Bugula neritina*. J. Nat. Prod. *70*, 67-74. https://doi.org/10.1021/np060361d.
9. Elshahawi, S.I., Trindade-Silva, A.E., Hanora, A., Han, A.W., Flores, M.S., Vizzoni, V., Schrago, C.G., Soares, C.A., Concepcion, G.P., Distel, D.L., et al. (2013). Boronated tartrolon antibiotic produced by symbiotic cellulose-degrading bacteria in shipworm gills. Proc. Natl. Acad. Sci. U.S.A. *110*, E295-304. https://doi.org/10.1073/pnas.1213892110.
10. Bhushan, A., Egli, P.J., Peters, E.E., Freeman, M.F., and Piel, J. (2019). Genome mining- and synthetic biology-enabled production of hypermodified peptides. Nat. Chem. *11*, 931-939. https://doi.org/10.1038/s41557-019-0323-9.
11. Rust, M., Helfrich, E.J.N., Freeman, M.F., Nanudorn, P., Field, C.M., Rückert, C., Kündig, T., Page, M.J., Webb, V.L., Kalinowski, J., et al. (2020). A multiproducer microbiome generates chemical diversity in the marine sponge *Mycale hentscheli*. Proc. Natl. Acad. Sci. U.S.A. *117*, 9508-9518. https://doi.org/10.1073/pnas.1919245117.
12. Storey, M.A., Andreassend, S.K., Bracegirdle, J., Brown, A., Keyzers, R.A., Ackerley, D.F., Northcote, P.T., and Owen, J.G. (2020). Metagenomic Exploration of the Marine Sponge *Mycale hentscheli* Uncovers Multiple Polyketide-Producing Bacterial Symbionts. mBio *11*, e02997-02919. https://doi.org/10.1128/mBio.02997-19.
13. Helfrich, E.J.N., and Piel, J. (2016). Biosynthesis of polyketides by *trans*-AT polyketide synthases. Nat. Prod. Rep. *33*, 231-316. https://doi.org/10.1039/C5NP00125K
14. Crits-Christoph, A., Diamond, S., Butterfield, C.N., Thomas, B.C., and Banfield, J.F. (2018). Novel soil bacteria possess diverse genes for secondary metabolite biosynthesis. Nature *558*, 440-444. https://doi.org/10.1038/s41586-018-0207-y.
15. Hemmerling, F., Meoded, R.A., Fraley, A.E., Minas, H.A., Dieterich, C.L., Rust, M., Ueoka, R., Jensen, K., Helfrich, E.J.N., Bergande, C., et al. (2022). Modular Halogenation, α-Hydroxylation, and Acylation by a Remarkably Versatile Polyketide Synthase. Angew. Chem. Int. Ed. *61*, e202116614. https://doi.org/10.1002/anie.202116614.
16. Meoded, R.A., Ueoka, R., Helfrich, E.J.N., Jensen, K., Magnus, N., Piechulla, B., and Piel, J. (2018). A Polyketide Synthase Component for Oxygen Insertion into Polyketide Backbones. Angew. Chem. Int. Ed. *57*, 11644-11648. 10.1002/anie.201805363.
17. Fraley, A.E., Dieterich, C.L., Mabesoone, M.F.J., Minas, H.A., Meoded, R.A., Hemmerling, F., and Piel, J. (2022). Structure of a Promiscuous Thioesterase Domain Responsible for Branching Acylation in Polyketide Biosynthesis. Angew. Chem. Int. Ed. *61*, e202206385. https://doi.org/10.1002/ange.202206385.

18. El-Sayed, A.K., Hothersall, J., Cooper, S.M., Stephens, E., Simpson, T.J., and Thomas, C.M. (2003). Characterization of the Mupirocin Biosynthesis Gene Cluster from *Pseudomonas fluorescens* NCIMB 10586. Chem. Biol. *10*, 419-430. https://doi.org/10.1016/S1074-5521(03)00091-7.
19. Mast, Y., Weber, T., Golz, M., Ort-Winklbauer, R., Gondran, A., Wohlleben, W., and Schinko, E. (2011). Characterization of the 'pristinamycin supercluster' of *Streptomyces pristinaespiralis*. Microb. Biotechnol. *4*, 192-206. https://doi.org/10.1111/j.1751-7915.2010.00213.x.
20. Flórez, L.V., Scherlach, K., Miller, I.J., Rodrigues, A., Kwan, J.C., Hertweck, C., and Kaltenpoth, M. (2018). An antifungal polyketide associated with horizontally acquired genes supports symbiont-mediated defense in *Lagria villosa* beetles. Nat. Commun. *9*, 1-10. https://doi.org/10.1038/s41467-018-04955-6.
21. Nguyen, T., Ishida, K., Jenke-Kodama, H., Dittmann, E., Gurgui, C., Hochmuth, T., Taudien, S., Platzer, M., Hertweck, C., and Piel, J. (2008). Exploiting the mosaic structure of *trans*-acyltransferase polyketide synthases for natural product discovery and pathway dissection. Nat. Biotechnol. *26*, 225-233. https://doi.org/10.1038/nbt1379.
22. Blin, K., Shaw, S., Kloosterman, A.M., Charlop-Powers, Z., van Wezel, G.P., Medema, M.H., and Weber, T. (2021). antiSMASH 6.0: improving cluster detection and comparison capabilities. Nucleic Acids Res. *49*, W29-W35. https://doi.org/10.1093/nar/gkab335.
23. Sayers, E.W., Cavanaugh, M., Clark, K., Pruitt, K.D., Schoch, C.L., Sherry, S.T., and Karsch-Mizrachi, I. (2021). GenBank. Nucleic Acids Res. *49*, D92-D96. https://doi.org/10.1093/nar/gkaa1023.
24. Blin, K., Shaw, S., Kautsar, S.A., Medema, M.H., and Weber, T. (2021). The antiSMASH database version 3: increased taxonomic coverage and new query features for modular enzymes. Nucleic Acids Res. *49*, D639-D643. https://doi.org/10.1093/nar/gkaa978.
25. Helfrich, E.J.N., Ueoka, R., Chevrette, M.G., Hemmerling, F., Lu, X., Leopold-Messer, S., Minas, H.A., Burch, A.Y., Lindow, S.E., Piel, J., and Medema, M.H. (2021). Evolution of combinatorial diversity in *trans*-acyltransferase polyketide synthase assembly lines across bacteria. Nat. Commun. *12*, 1422. https://doi.org/10.1038/s41467-021-21163-x.
26. Helfrich, E.J.N., Ueoka, R., Dolev, A., Rust, M., Meoded, R.A., Bhushan, A., Califano, G., Costa, R., Gugger, M., Steinbeck, C., et al. (2019). Automated structure prediction of *trans*-acyltransferase polyketide synthase products. Nat. Chem. Biol. *15*, 813-821. https://doi.org/10.1038/s41589-019-0313-7.
27. CHEMnetBASE. Dictionary of Natural Products (2022). http://dnp.chemnetbase.com/. accessed: June 18. 2022
28. PubChem (2022). https://pubchem.ncbi.nlm.nih.gov/. accessed: June 18. 2022
29. Reaxys (2022). https://www.reaxys.com/. accessed: June 18. 2022
30. Fukunaga, Y., Kurahashi, M., Yanagi, K., Yokota, A., and Harayama, S. (2008). *Acanthopleuribacter pedis* gen. nov., sp. nov., a marine bacterium isolated from a chiton, and description of *Acanthopleuribacteraceae* fam. nov., *Acanthopleuribacterales* ord. nov., *Holophagaceae* fam. nov., *Holophagales* ord. nov. and *Holophagae* classis nov. in the phylum '*Acidobacteria*'. Int. J. Syst. Evol. Microbiol. *58*, 2597-2601. https://doi.org/10.1099/ijs.0.65589-0.
31. Wang, G., Li, Y., Liu, J., Chen, B., Su, H., Liang, J., Huang, W., and Yu, K. (2022). Comparative Genomics Reveal the Animal-Associated Features of the *Acanthopleuribacteraceae* Bacteria, and Description of *Sulfidibacter corallicola* gen. nov., sp., nov. Front. Microbiol. *13*, 778535. https://doi.org/10.3389/fmicb.2022.778535.
32. Capon, R.J., Skene, C., Liu, E.H., Lacey, E., Gill, J.H., Heiland, K., and Friedel, T. (2004). Esmodil: An Acetylcholine Mimetic Resurfaces in a Southern Australian Marine Sponge *Raspailia* (*Raspailia*) sp. Nat. Prod. Res. *18*, 305-309. https://doi.org/10.1080/14786410310001620619.
33. Wang, M., Carver, J.J., Phelan, V.V., Sanchez, L.M., Garg, N., Peng, Y., Nguyen, D.D., Watrous, J., Kapono, C.A., Luzzatto-Knaan, T., et al. (2016). Sharing and community curation of mass spectrometry data with Global Natural Products Social Molecular Networking. Nat. Biotechnol. *34*, 828-837. https://doi.org/10.1038/nbt.3597.
34. Weissman, K.J. (2017). Polyketide stereocontrol: a study in chemical biology. Beilstein J. Org. Chem. *13*, 348-371. https://doi.org/10.3762/bjoc.13.39.
35. Smith III, A.B., Verhoest, P.R., Minbiole, K.P., and Schelhaas, M. (2001). Total Synthesis of (+)-Phorboxazole A. J. Am. Chem. Soc. *123*, 4834-4836. https://doi.org/10.1021/ja0105055.

36. Bisang, C., Long, P.F., Corte´s, J., Westcott, J., Crosby, J., Matharu, A.-L., Cox, R.J., Simpson, T.J., Staunton, J., and Leadlay, P.F. (1999). A chain initiation factor common to both modular and aromatic polyketide synthases. Nature *401*, 502-505. https://doi.org/10.1038/46829.
37. Ishihara, H., Martin, B.L., Brautigan, D.L., Karaki, H., Ozaki, H., Kato, Y., Fusetani, N., Watabe, S., Hashimoto, K., Uemura, D., and Hartshome, D.J. (1989). Calyculin A and Okadaic Acid: Inhibitors of Protein Phosphatase activity. Biochem. Biophys. Res. Commun. *159*, 871-877. https://doi.org/10.1016/0006-291X(89)92189-X.
38. Wakimoto, T., Egami, Y., and Abe, I. (2016). Calyculin: Nature's way of making the sponge-derived cytotoxin. Nat Prod Rep *33*, 751-760. https://doi.org/10.1039/c5np00123d.
39. Cohen, P., Holmes, C.F.B., and Tsukitanic, Y. (1990). Okadaic acid: a new probe for the study of cellular regulation. Trends Biochem. Sci. *15*, 98-102. https://doi.org/10.1016/0968-0004(90)90192-E.
40. Kehraus, S., König, G.M., and Wright, A.D. (2002). A New Cytotoxic Calyculinamide Derivative, Geometricin A, from the Australian Sponge *Luffariella geometrica*. J. Nat. Prod. *65*, 1056-1058. https://doi.org/10.1021/np010544u.
41. Edrada, R.A., Ebel, R., Supriyono, A., Wray, V., Schupp, P., Steube, K., van Soest, R., and Proksch, P. (2002). Swinhoeiamide A, a New Highly Active Calyculin Derivative from the Marine Sponge *Theonella swinhoei*. J. Nat. Prod. *65*, 1168-1172. https://doi.org/10.1021/np020049d.
42. Blin, K., Shaw, S., Steinke, K., Villebro, R., Ziemert, N., Lee, S.Y., Medema, M.H., and Weber, T. (2019). AntiSMASH 5.0: updates to the secondary metabolite genome mining pipeline. Nucleic Acids Res. *47*, W81-W87. https://doi.org/10.1093/nar/gkz310.
43. Skinnider, M.A., Johnston, C.W., Gunabalasingam, M., Merwin, N.J., Kieliszek, A.M., MacLellan, R.J., Li, H., Ranieri, M.R.M., Webster, A.L.H., Cao, M.P.T., et al. (2020). Comprehensive prediction of secondary metabolite structure and biological activity from microbial genome sequences. Nat. Commun. *11*, 6058. https://doi.org/10.1038/s41467-020-19986-1.
44. SciFinder-n (2023). scifinder-n.cas.org/. accessed: August 28. 2023
45. Tajima, H., Wakimoto, T., Takada, K., Ise, Y., and Abe, I. (2014). Revised Structure of Cyclolithistide A, a Cyclic Depsipeptide from the Marine Sponge *Discodermia japonica*. J. Nat. Prod. *77*, 154-158. https://doi.org/10.1021/np400668k.
46. Clark, D.P., Carroll, J., Naylor, S., and Crews, P. (1998). An Antifungal Cyclodepsipeptide, Cyclolithistide A, from the Sponge *Theonella swinhoei*. J. Org. Chem. *63*, 8757-8764. https://doi.org/10.1021/jo980758p.
47. Capon, R.J., Ford, J., Lacey, E., Gill, J.H., Heiland, K., and Friedel, T. (2002). Phoriospongin A and B: Two New Nematocidal Depsipeptides from the Australian Marine Sponges *Phoriospongia* sp. and *Callyspongia bilamellata*. J. Nat. Prod. *65*, 358-363. https://doi.org/10.1021/np010329d.
48. Fujimori, D.G. (2013). Radical SAM-mediated methylation reactions. Curr. Opin. Chem. Biol. *17*, 597-604. https://doi.org/10.1016/j.cbpa.2013.05.032.
49. Kelley, L.A., Mezulis, S., Yates, C.M., Wass, M.N., and Sternberg, M.J. (2015). The Phyre2 web portal for protein modeling, prediction and analysis. Nat. Protoc. *10*, 845-858. 10.1038/nprot.2015-053.
50. Wirtz, D.A., Schneberger, N., Klöppel, S., Richarz, R., Geyer, M., König, G.M., Hagelueken, G., and Crüsemann, M. (2023). Adenylation Domain-Guided Recruitment of *Trans*-Acting Nonheme Monooxygenases in Nonribosomal Peptide Biosynthesis. ACS Chem. Biol. *18*, 1748-1759. https://doi.org/10.1021/acschembio.3c00106.
51. Makris, T.M., Knoot, C.J., Wilmot, C.M., and Lipscomb, J.D. (2013). Structure of a Dinuclear Iron Cluster-Containing β-Hydroxylase Active in Antibiotic Biosynthesis. Biochemistry *52*, 6662-6671. https://doi.org/10.1021/bi400845b.
52. Hoye, T.R., Jeffrey, C.S., and Shao, F. (2007). Mosher ester analysis for the determination of absolute configuration of stereogenic (chiral) carbinol carbons. Nat. Protoc. *2*, 2451-2458. https://doi.org/10.1038/nprot.2007.354.
53. Smith III, A.B., Liu, Z., Hogan, A.-M.L., Dalisay, D.S., and Molinski, T.F. (2009). Hemi-Phorboxazole A: Structure Confirmation, Analogue Design and Biological Evaluation. Org. Lett. *11*, 3766-3769. https://doi.org/10.1021/ol9014317.
54. Uckun, F.M., and Forsyth, C.J. (2001). Anticancer Activity of Synthetic Analogues of the Phorboxazoles. Bioorg. Med. Chem. Lett. *11*, 1181-1183. https://doi.org/10.1016/S0960-894X(01)00191-3.
55. Petras, D., Kerwat, D., Pesic, A., Hempel, B.F., von Eckardstein, L., Semsary, S., Arasté, J., Marguerettaz, M., Royer, M., Cociancich, S., and Süssmuth, R.D. (2016). The *O*-Carbamoyl-Transferase Alb15 Is Responsible for the Modification of

Albicidin. ACS Chem. Biol. *11*, 1198-1204. https://doi.org/10.1021/acschembio.5b01001.
56. Hooper, D.C., Wolfson, J.S., McHugh, G.L., Winters, M.B., and Swartz, M.N. (1982). Effects of Novobiocin, Coumermycin Al, Clorobiocin, and Their Analogs on *Escherichia coli* DNA Gyrase and Bacterial Growth. Antimicrob. Agents Chemother. *22*, 662-671. https://doi.org/10.1128/AAC.22.4.662.
57. Kato, Y., Fusetani, N., Matsunaga, S., and Hashimoto, K. (1986). Calyculin A, a Novel Antitumor Metabolite from the Marine Sponge *Discodermia calyx*. J. Am. Chem. Soc. *108*, 2780-2781. https://doi.org/10.1021/ja00270a061.
58. Matsunaga, S., Wakimoto, T., and Fusetani, N. (1997). Isolation of Four New Calyculins from the Marine Sponge *Discodermia calyx*. J. Org. Chem. *62*, 2640-2642. https://doi.org/10.1021/jo961746b.
59. Paoli, L., Ruscheweyh, H.J., Forneris, C.C., Hubrich, F., Kautsar, S., Bhushan, A., Lotti, A., Clayssen, Q., Salazar, G., Milanese, A., et al. (2022). Biosynthetic potential of the global ocean microbiome. Nature *607*, 111-118. https://doi.org/10.1038/s41586-022-04862-3.
60. Terlouw, B.R., Blin, K., Navarro-Munoz, J.C., Avalon, N.E., Chevrette, M.G., Egbert, S., Lee, S., Meijer, D., Recchia, M.J.J., Reitz, Z.L., et al. (2023). MIBiG 3.0: a community-driven effort to annotate experimentally validated biosynthetic gene clusters. Nucleic Acids Res. *51*, D603-D610. https://doi.org/10.1093/nar/gkac1049.
61. Mavrodi, O.V., Jung, C.M., Eberly, J.O., Hendry, S.V., Namjilsuren, S., Biber, P.D., Indest, K.J., and Mavrodi, D.V. (2018). Rhizosphere Microbial Communities of *Spartina alterniflora* and *Juncus roemerianus* From Restored and Natural Tidal Marshes on Deer Island, Mississippi. Front. Microbiol. *9*, 1-13. https://doi.org/10.3389/fmicb.2018.03049.
62. Jones, R.T., Robeson, M.S., Lauber, C.L., Hamady, M., Knight, R., and Fierer, N. (2009). A comprehensive survey of soil acidobacterial diversity using pyrosequencing and clone library analyses. ISME Journal *3*, 442-453. https://doi.org/10.1038/ismej.2008.127.
63. Janssen, P.H. (2006). Identifying the dominant soil bacterial taxa in libraries of 16S rRNA and 16S rRNA genes. Appl. Environ. Microbiol. *72*, 1719-1728. https://doi.org/10.1128/AEM.72.3.1719-1728.2006.
64. Kielak, A.M., Barreto, C.C., Kowalchuk, G.A., van Veen, J.A., and Kuramae, E.E. (2016). The Ecology of *Acidobacteria*: Moving beyond Genes and Genomes. Front. Microbiol. *7*, 744. https://doi.org/10.3389/fmicb.2016.00744.
65. Crits-Christoph, A., Diamond, S., Al-Shayeb, B., Valentin-Alvarado, L., and Banfield, J.F. (2022). A widely distributed genus of soil Acidobacteria genomically enriched in biosynthetic gene clusters. ISME Commun. *2*. https://doi.org/10.1038/s43705-022-00140-5.
66. Kautsar, S.A., van der Hooft, J.J.J., de Ridder, D., and Medema, M.H. (2021). BiG-SLiCE: A highly scalable tool maps the diversity of 1.2 million biosynthetic gene clusters. Gigascience *10*, 1-17. https://doi.org/10.1093/gigascience/giaa154.
67. Andrianasolo, E.H., Gross, H., Goeger, D., Musafija-Girt, M., McPhail, K., Leal, R.M., Mooberry, S.L., and Gerwick, W.H. (2005). Isolation of Swinholide A and Related Glycosylated Derivatives from Two Field Collections of Marine Cyanobacteria. Org. Lett. *7*, 1375-1378. https://doi.org/10.1021/ol050188x.
68. Strobel, G., Li, J.-Y., Sugawara, F., Koshino, H., Harper, J., and Hess, W.M. (1999). Oocydin A, a chlorinated macrocyclic lactone with potent anti-oomycete activity from *Serratia marcescens*. Microbiology *145*, 3557-3564. https://doi.org/10.1099/00221287-145-12-3557.
69. Suzumura, K.-i., Takahashi, I.M., Hisao Nagai, Koji Setiawan, Boeqjamin , Rantiatmodjo, R.M., and Suzuki, K.-i.N., Noriaki (1997). Structural Elucidation of YM-75518, A Novel Antifungal Antibiotic Isolated from *Pseudomonas* sp. Q38009. Tetrahedron *38*, 7573-7576. https://doi.org/10.1016/S0040-4039(97)01785-1.
70. Ueoka, R., Meoded, R.A., Gran-Scheuch, A., Bhushan, A., Fraaje, M.W., and Piel, J. (2020). Genome Mining of Oxidation Modules in *trans*-Acyltransferase Polyketide Synthases Reveals a Culturable Source for Lobatamides. Angew. Chem. Int. Ed. *59*, 7761-7765. https://doi.org/10.1002/anie.201916005.
71. Tsukimoto, M., Nagaoka, M., Shishido, Y., Fujimoto, J., Nishisaka, F., Matsumoto, S., Harunari, E., Imada, C., and Matsuzaki, T. (2011). Bacterial Production of the Tunicate-Derived Antitumor Cyclic Depsipeptide Didemnin B. J. Nat. Prod. *74*, 2329-2331. https://doi.org/10.1021/np200543z.
72. Hoffmann, T., Müller, S., Nadmid, S., Garcia, R., and Müller, R. (2013). Microsclerodermins from Terrestrial Myxobacteria: An Intriguing Biosynthesis Likely Connected to a Sponge Symbiont. J. Am. Chem. Soc. *135*, 16904-16911. https://doi.org/10.1021/ja4054509.

73. Wenzel, S.C., Hoffmann, H., Zhang, J., Debussche, L., Haag-Richter, S., Kurz, M., Nardi, F., Lukat, P., Kochems, I., Tietgen, H., et al. (2015). Production of the Bengamide Class of Marine Natural Products in Myxobacteria: Biosynthesis and Structure-Activity Relationships. Angew. Chem. Int. Ed. *54*, 15560-15564. https://doi.org/10.1002/anie.201508277.
74. Freeman, M.F., Gurgui, C., Helf, M.J., Morinaka, B.I., Uria, A.R., Oldham, N.J., Sahl, H.-G., Matsunaga, S., and Piel, J. (2012). Metagenome Mining Reveals Polytheonamides as Posttranslationally Modified Ribosomal Peptides. Science *338*, 387-390. https://doi.org/10.1126/science.1226121.

Figure Captions

Figure 1. Examples of complex polyketides from marine invertebrates.

Some of these compounds (**3**-**6**) have been linked to symbiotic bacteria while for others (**1**, **2**) the producers and biosynthetic genes remain elusive.

Figure 2. Global analysis of bacterial *trans*-AT PKS gene clusters and identification of a talented producer taxon.

(A) *Trans*-AT PKSs gene clusters in genomes published in GenBank[23] were analyzed with the TransPACT tool.[25] TransPACT predicts for each PKS a series of polyketide moieties as substrates of all KSs and represents them as color-coded patterns. The phylogenetic tree indicates the relatedness of PKS BGCs based on their KS patterns[25] (see Supplemental Information and GitHub for details on visualization). This visualization allows rapid dereplication of PKSs similar to already characterized ones (annotated for some examples, e.g., bacillaene), identification of rare orphan PKSs, and identification of alternative producers for BGCs of interest (e.g., a cultivated calyculin producer). Red branches indicate BGCs found in Acidobacteria, blue branches indicate the *pho* BGC in *A. pedis* and the *phb* BGC in *S. corallicola*, and the orange branch indicates the *cly* cluster in *A. pedis* as well as the *cal* BGC in '*Ca.* Entotheonella sp.'. The legend indicates the predicted KS substrates. KSs individually assignable to pyran units, oxazole rings, chain branching, and oxygen insertion are summarized in the KS legend as "specialized" (Supplemental Information).

(B) Expanded view of a tree section containing the *pho*, *phb*, *cly*, and *cal* BGCs.

(C) KS domain sequences of the Acidobacterial BGCs.

(D) AntiSMASH analysis of the two bacteria harboring the *pho*, *phb*, *cly*, and *cal* PKSs. Both strains belong to the family *Acanthopleuribacteraceae*, have large genomes, and contain around 40 BGCs, suggesting a talented producer taxon within the phylum Acidobacteria. RiPP: Ribosomally synthesized and post-translationally modified peptide.

Figure 3. Products of the *pho trans*-AT PKS isolated from *A. pedis*.

(A) Top: TransATor-based structural prediction of the *pho* BGC product. Bottom: structure of sponge-derived phorboxazole A (**1**). Moieties shared by both structures are highlighted in blue.

(B) Phorbactazoles A-F (**7-12**) isolated in this study. The relative configuration (marked by an asterisk) of rings A-D in **7** was assigned by NOESY correlations (Figure S11). The absolute configuration of the remaining hydroxy group-bearing carbon centers was suggested by analysis of KR and KS domains (Table S2), with a relative configuration matching the NMR data. The only exception was C-32, for which bioinformatic data were contradictory but for which the configuration could be determined by NMR. Due to different atom priorities of C-17 and C-19 the assignment of C-18 in **8** and **10** (18*S*) is inverted to that in **7**, **9**, **11**, **12** (18*R*).

Figure 4. Proposed biosynthesis of phorbactazoles by the *pho trans*-AT PKS.

(A) Map of the *pho* biosynthetic locus.

(B) Biosynthetic model of the phorbactazole assembly line. The predicted flavin-dependent oxidoreductase PhoL might be responsible for α-hydroxylation in modules 17 and 21. The glycosyltransferase PhoF and the *O*-carbamoyltransferase PhoM would generate the final products. Suggested configurations of hydroxy groups based on bioinformatic prediction, are shown above KR domains. The KR-based prediction upstream of KS9 is opposite of what the KS and NOESY data suggest. OX: oxygenase, Cy: cyclization domain, A: adenylation domain, DH: dehydratase domain. Filled black circles: acyl or peptidyl carrier protein.

Figure 5. Additional polyketides and depsipeptides isolated from *A. pedis* and related compounds from sponges.

(A) 21-Methoxy calyculinamide A (**13**) of the *cly trans*-AT PKS in *A. pedis* (left) and the structurally related previously reported sponge-derived calyculinamide A (**14**) and calyculin (**3**) (right). The relative configuration (indicated by an asterisk) of the spiro system in **13** was determined by NMR (Supplemental Information), the absolute configuration is suggested by PKS domain analyses and matches that of **14** with the exception of C-21. Several stereocenters of **13** could not be determined by NMR or predicted from the PKS sequence.

(B) The depsipeptides acidobactamide A-C (**15**-**17**) are putatively biosynthesized by the *aba* NRPS-PKS hybrid (Figure S52) and were isolated from the cell pellet of *A. pedis*. The structure features a macrocycle and multiple unusual building blocks. A nonmethylated Admha residue, Adha, is also present in sponge derived depsipeptides such as cyclolithistide A (**18**), embedded in a shared three-residue moiety highlighted in purple. Ddmpha: 6-diamino-5,7-dihydroxy-7-(4-methoxyphenyl)heptanoic acid; Hppa: 2-hydroxy-3-phenylpropanoic acid; Admha: 4-amino-3,5-dihydroxy-2-methylhexanoic acid. The absolute configuration was assigned using the modified Mosher method (Supplemental Information).[52] Chemical shift differences were only observed on one site of the plane for the hydroxy group of carbon C-45, possibly because of the close proximity of MTPA substituents.

Figure 6. Characterized and uncharacterized *Acanthopleuribacteraceae* are talented and diverse natural product producers.

(A) Collection and metagenome sequencing of a *Millepora* coral collected by the *Tara Pacific* expedition near Tobi island (2°59'54.5"N 131°07'31.4"E; Republic of Palau; sample ID: TARA_CO-0003230). Inset: Photo of *Millepora platyphylla.*

(B) Phylogenetic analysis based on a single-copy marker gene (COG0012; Supplementary Information) resolves the evolutionary relationships between *A. pedis*, *S. corallicola*, and a previously unreported coral-associated Acanthopleuribacteraceae strain for which a metagenome assembled genome was reconstructed. GTDBTk annotations (Supplementary Information) indicate that all three genomes belong to different genera of the Acanthopleuribacteraceae family.

(C) AntiSMASH analysis reveals that the *M. platyphylla*-associated *Acantipleuribacteraceae* member is as chemically rich as *A. pedis* and *S. corallicola* and features an impressive number of biosynthetic gene clusters, including multiple *trans*-AT PKS BGCs (only BGCs longer than 5 kb were included in the analysis).

(D) *Trans*PACT analysis indicates that the *trans*-AT PKSs found in *Acantipleuribacteraceae* are diverse and distinct when compared to the BGCs deposited in MIBiG[60]. For this analysis, clusters that contained one or more PKSs with at least two KS domains and no *cis*-AT domains were extracted from the MIBiG database. The legend refers to the inner tracks. The legend referring to the outer KS phylogenies can be found in Figure 2.

(E) Two examples of architecturally unusual *trans*-AT PKS-NRPS BGCs from the *Millepora*-associated strain. The assembly lines comprise 10 and 24 modules, respectively, with a repeated occurrence of domains of unknown function (DUF) adjacent to pyridoxal phosphate-(PLP-)dependent domains.

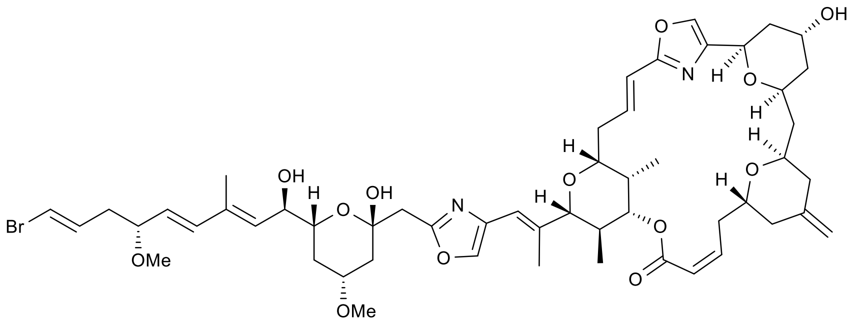

phorboxazole A (**1**)
producer unkown; isolated from a *Phorbas* sp. sponge

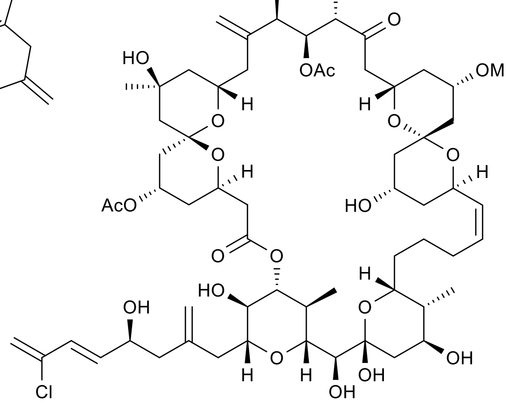

spongistatin 1 (**2**)
producer unknown; isolated from a *Spongia* sp. sponge

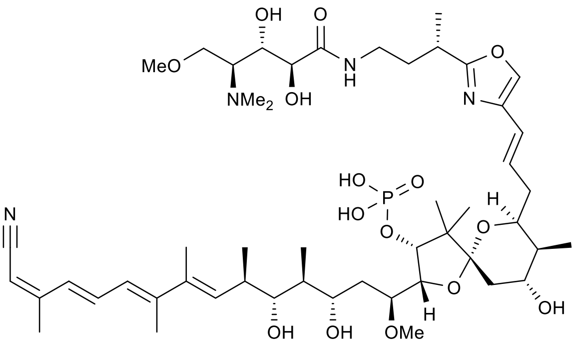

calyculin A (**3**)
Candidatus Entotheonella sp.; symbiont of the sponge *Discodermia calyx*

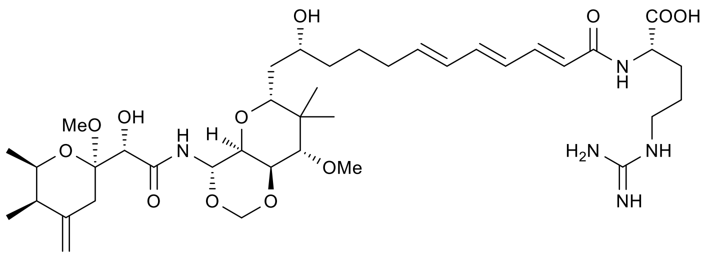

onnamide A (**4**)
Candidatus Entotheonella sp.; symbiont of the sponge *Theonella* sp.

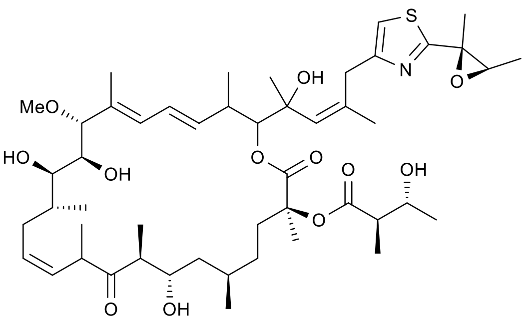

patellazole B (**5**)
Candidatus Endolissoclinum faulkneri; symbiont of the tunicate *Lissoclinum patella*

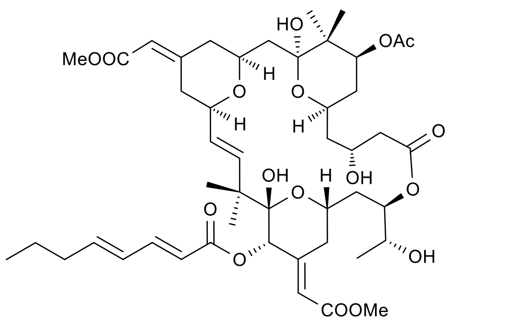

bryostatin 1 (**6**)
Candidatus Endobugula sertula; symbiont of the bryozoan *Bugula neritina*

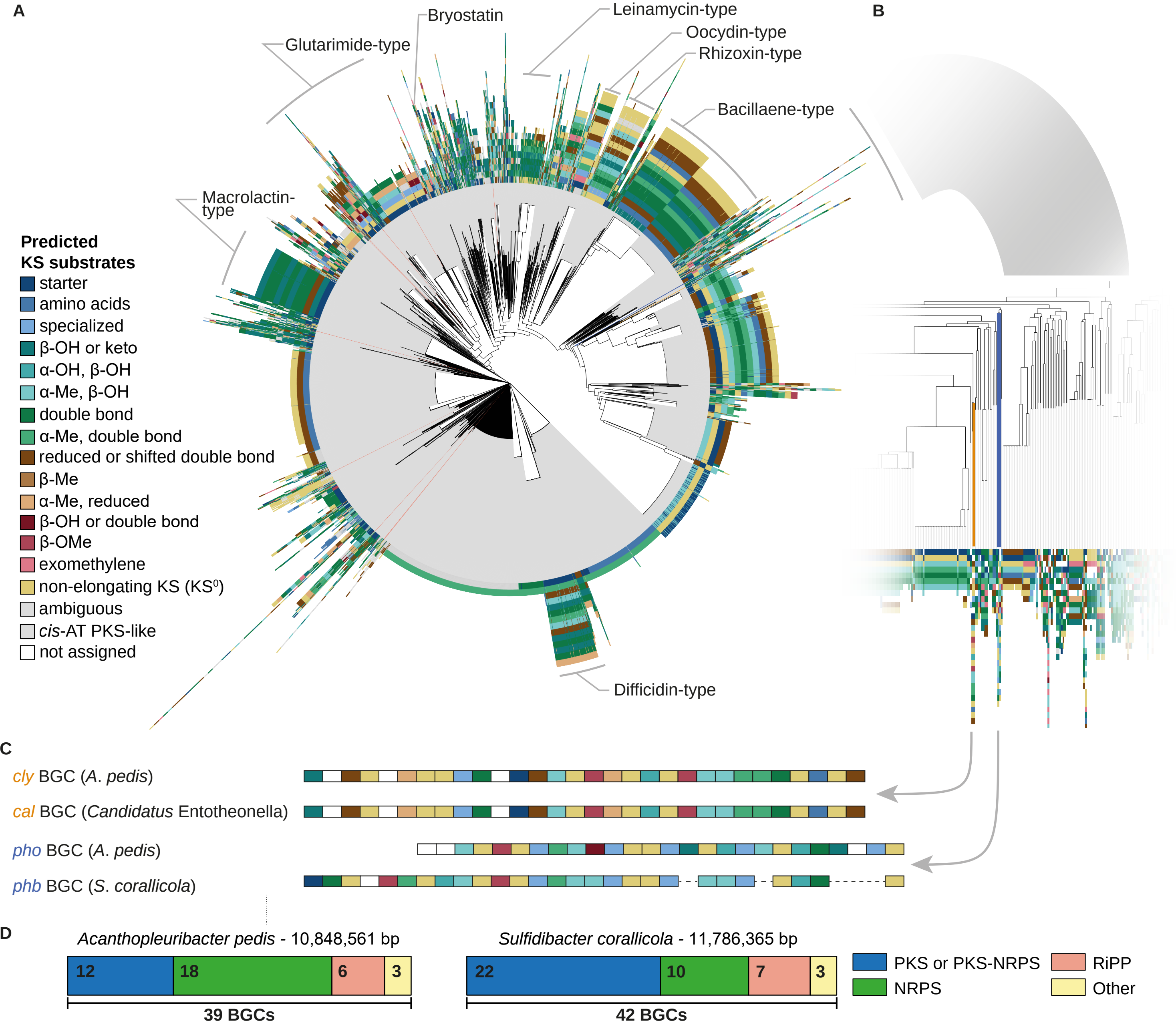
A
B
Glutarimide-type
Bryostatin
Leinamycin-type
Oocydin-type
Rhizoxin-type
Bacillaene-type
Macrolactin-type
Difficidin-type
Predicted KS substrates
starter
amino acids
specialized
β-OH or keto
α-OH, β-OH
α-Me, β-OH
double bond
α-Me, double bond
reduced or shifted double bond
β-Me
α-Me, reduced
β-OH or double bond
β-OMe
exomethylene
non-elongating KS (KS⁰)
ambiguous
cis-AT PKS-like
not assigned
C
cly BGC (A. pedis)
cal BGC (Candidatus Entotheonella)
pho BGC (A. pedis)
phb BGC (S. corallicola)
D
Acanthopleuribacter pedis - 10,848,561 bp
12
18
6
3
39 BGCs
Sulfidibacter corallicola - 11,786,365 bp
22
10
7
3
42 BGCs
PKS or PKS-NRPS
NRPS
RiPP
Other

A

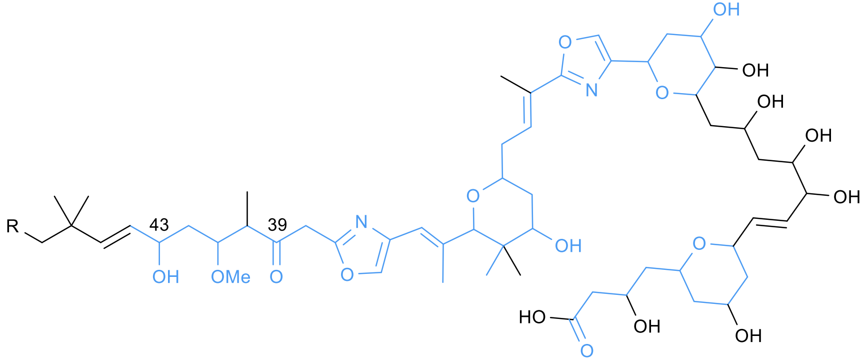

automated TransATor prediction of PhoA-E

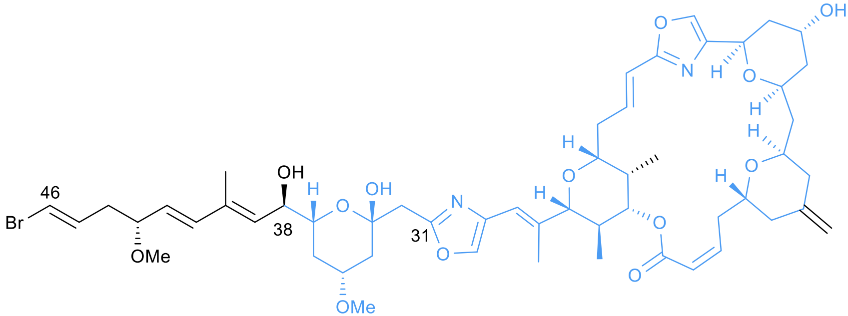

phorboxazole A (**1**)

B

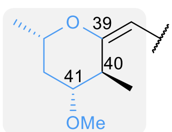

phorbactazole E (**11**)
R¹ = $CONH_2$ R² = D-glucose

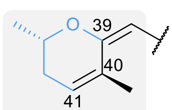

phorbactazole F (**12**)
R¹ = $CONH_2$ R² = D-glucose

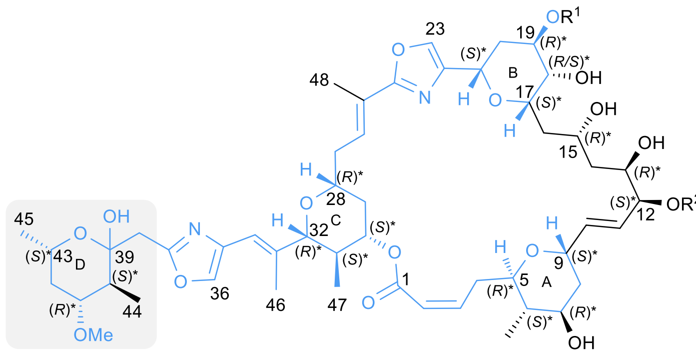

phorbactazole A (**7**) R¹ = $CONH_2$ R² = H
phorbactazole B (**8**) R¹ = H R² = H
phorbactazole C (**9**) R¹ = $CONH_2$ R² = D-glucose
phorbactazole D (**10**) R¹ = H R² = D-glucose

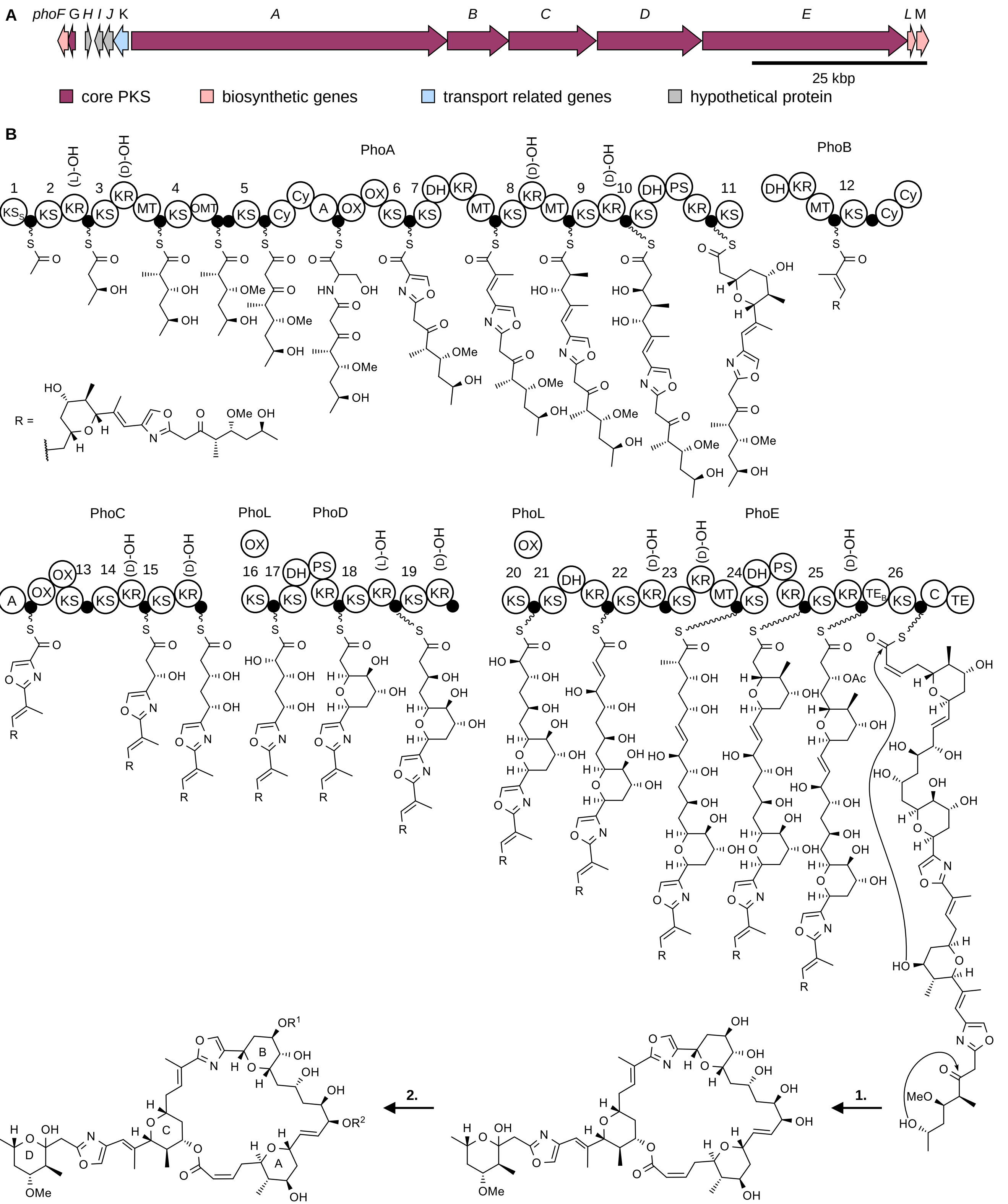

phorbactazole A (**7**) R_1 = $CONH_2$ R_2 = H
phorbactazole B (**8**) R_1 = H R_2 = H
phorbactazole C (**9**) R_1 = $CONH_2$ R_2 = D-glucose
phorbactazole D (**10**) R_1 = H R_2 = D-glucose

1. release, cyclization, hemiketal formation
2. PhoF (glycosylation) and PhoM (*O*-carbamoylation)

A

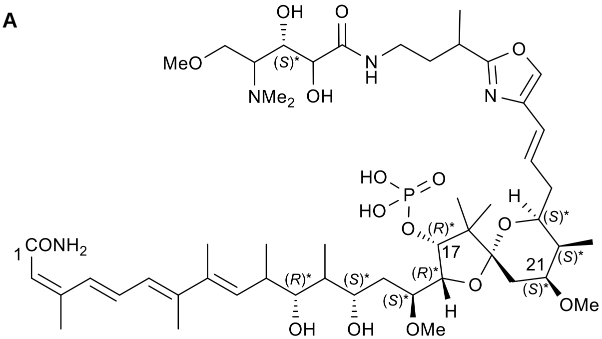

21-methoxy calyculinamide A (**13**)
isolated from *Acanthopleuribacter pedis*

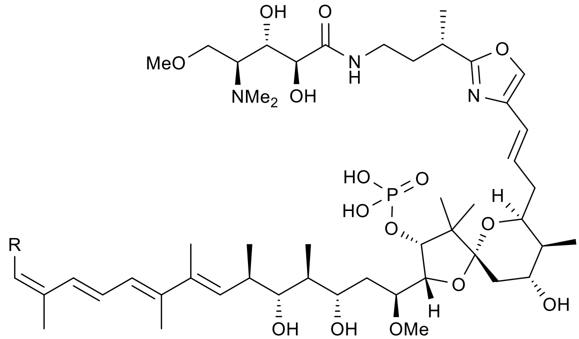

calyculin A (**3**) R = CN
calyculinamide A (**14**) R = $CONH_2$
isolated from the sponge *Discodermia calyx*

B

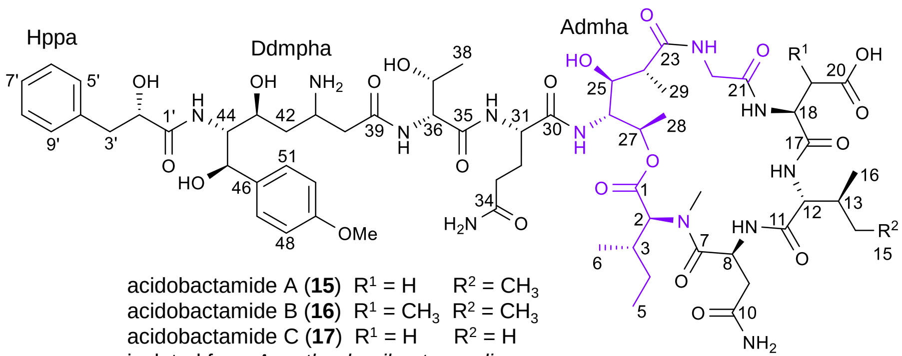

acidobactamide A (**15**) $R^1 = H$ $R^2 = CH_3$
acidobactamide B (**16**) $R^1 = CH_3$ $R^2 = CH_3$
acidobactamide C (**17**) $R^1 = H$ $R^2 = H$
isolated from *Acanthopleuribacter pedis*

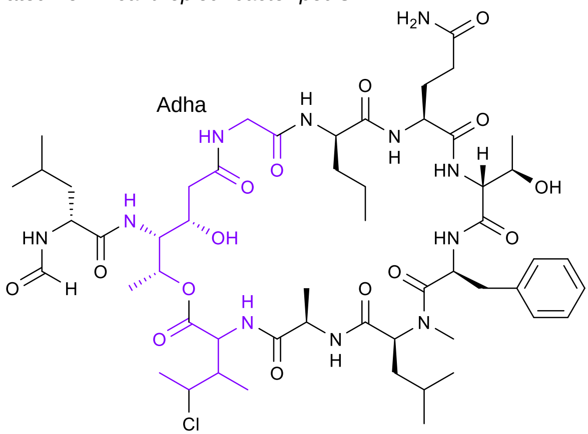

cyclolithistide A (**18**)
isolated from the sponges *Discodermia japonica* and *Theonella swinhoei*

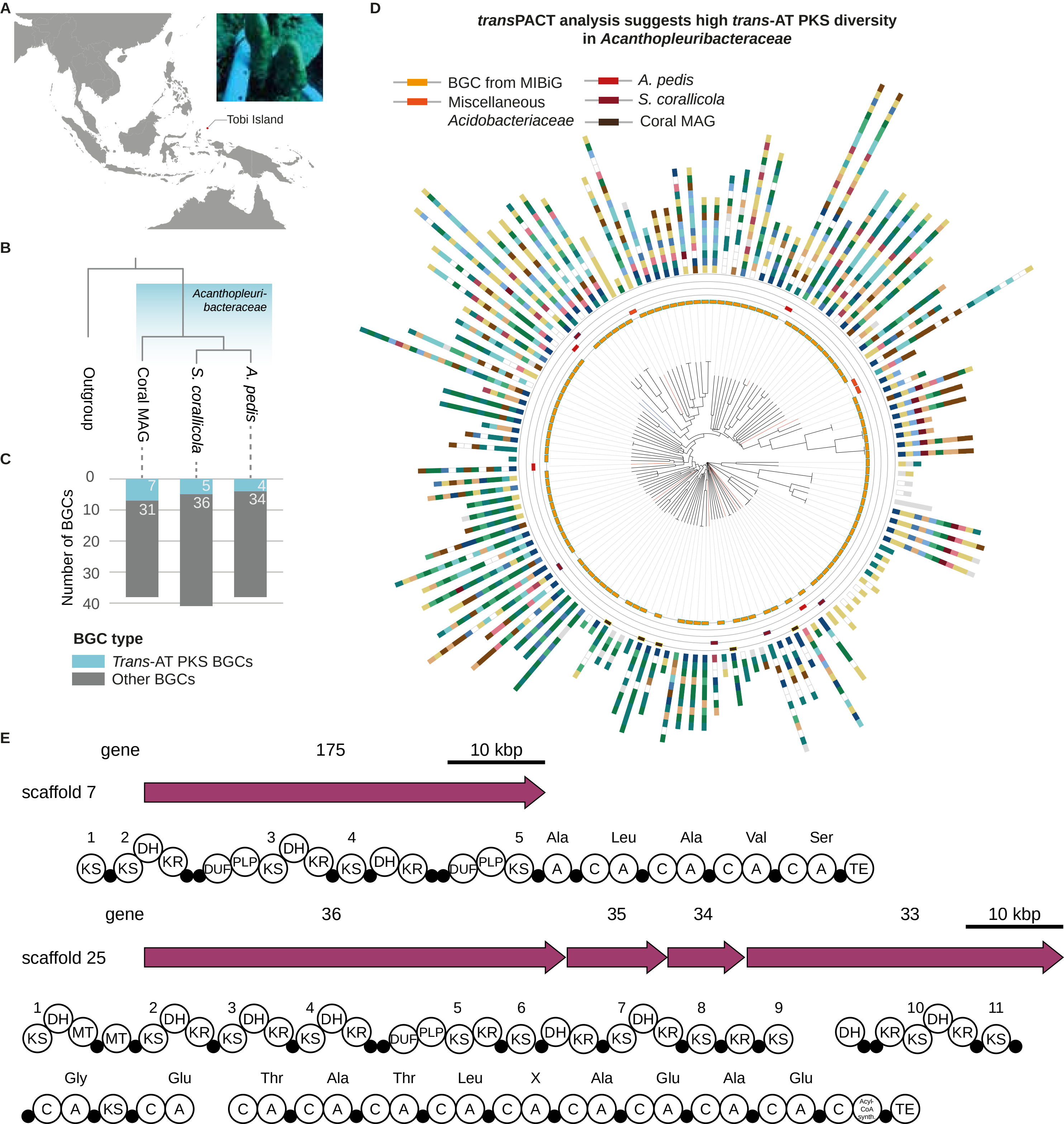

A
Tobi Island
B
Acanthopleuri-bacteraceae
Outgroup
Coral MAG
S. corallicola
A. pedis
C
Number of BGCs
0
10
20
30
40
7
31
5
36
4
34
BGC type
Trans-AT PKS BGCs
Other BGCs
D
transPACT analysis suggests high trans-AT PKS diversity in Acanthopleuribacteraceae
BGC from MIBiG
Miscellaneous Acidobacteriaceae
A. pedis
S. corallicola
Coral MAG
E
gene
175
10 kbp
scaffold 7
1 2 3 4 5
Ala Leu Ala Val Ser
KS KS DH KR DUF PLP KS DH KR KS DH KR DUF PLP KS A C A C A C A C A TE
gene
36
35
34
33
10 kbp
scaffold 25
1 2 3 4 5 6 7 8 9 10 11
KS DH MT MT KS DH KR KS DH KR KS DH KR DUF PLP KS KR KS DH KR KS DH KR KS KR KS DH KR KS DH KR KS
Gly Glu Thr Ala Thr Leu X Ala Glu Ala Glu
C A KS C A C A C A C A C A C A C A C A C A C A C Acyl-CoA synth. TE

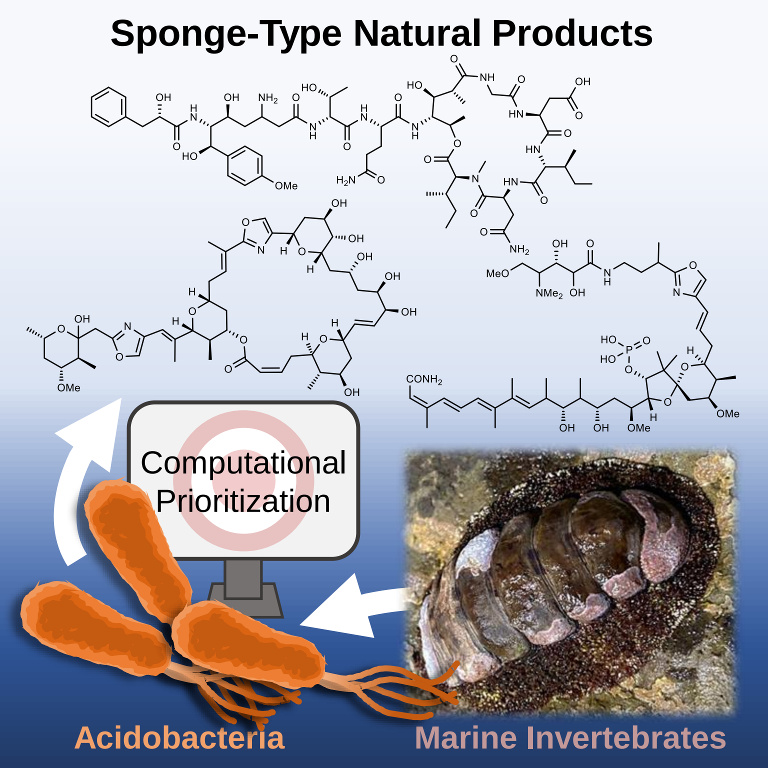

Sponge-Type Natural Products
Computational
Prioritization
Acidobacteria
Marine Invertebrates